ISSN 0036-0244, Russian Journal of Physical Chemistry A, 2018, Vol. 92, No. 3, pp. 430–437. © Pleiades Publishing, Ltd., 2018.
Original Russian Text © V.I. Lomonosov, Yu.A. Gordienko, M.Yu. Sinev, V.A. Rogov, V.A. Sadykov, 2018, published in Zhurnal Fizicheskoi Khimii, 2018, Vol. 92, No. 3, pp. 386–394.

CHEMICAL KINETICS AND CATALYSIS

Thermochemical Properties of the Lattice Oxygen in W,Mn-Containing Mixed Oxide Catalysts for the Oxidative Coupling of Methane

V. I. Lomonosov[a], Yu. A. Gordienko[a], M. Yu. Sinev[a,*], V. A. Rogov[b,c], and V. A. Sadykov[b,c]

[a] *Semenov Institute of Chemical Physics, Russian Academy of Sciences, Moscow, 119991 Russia*
[b] *Boreskov Institute of Catalysis, Siberian Branch, Russian Academy of Sciences, Novosibirsk, 630090 Russia*
[c] *Novosibirsk State University, Novosibirsk, 630090 Russia*
**e-mail: mysinev@rambler.ru*

Received May 22, 2017

Abstract—Mixed $NaWMn/SiO_2$ oxide, samples containing individual components (Na, W, Mn) and their double combinations (Na–W, Na–Mn, W–Mn) supported on silica were studied by temperature programmed reduction (TPR) and desorption (TPD), and heat flow calorimetry during their reoxidation with molecular oxygen in pulse mode. The $NaWMn/SiO_2$ mixed oxide was shown to contain two different types of reactive lattice oxygen. The weakly-bonded oxygen can be reversibly released from the oxide in a flow of inert gas in the temperature range of 575–900°C, while the strongly-bonded oxygen can be removed during the reduction of the sample with hydrogen at 700–900°C. The measured thermal effect of oxygen consumption for these two oxygen forms are 185 and 350 kJ/mol, respectively. The amount of oxygen removed at reduction (~443 μmol/g) considerably exceeded the amount desorbed in an inert gas flow (~56 μmol/g). The obtained results suggest that the reversible oxygen desorption is due to the redox process in which manganese ions are involved, while during the temperature programmed reduction, mainly oxygen bonded with tungsten is removed.

Keywords: methane, oxidative coupling, oxide catalysts, lattice oxygen

DOI: 10.1134/S0036024418030147

INTRODUCTION

The revival of the interest of both scientists and engineers to the direct ethylene synthesis via the oxidative coupling of methane (OCM) has been observed over the last few years. A great interest to this process in the early 1980s was initiated by the publication [1]. In the beginning, the main efforts were focused on the development of active and selective catalytic systems. Detailed reviews and analysis of publications dedicated to the OCM catalyst selection and characterization can be found in [2, 3]. The effective OCM catalysts are almost exclusively represented by various individual and mixed oxides, mainly of non-transition metals. However, the most effective catalytic system (from the point of view of the maximum achievable yield of C_2-hydrocarbons) known to date is $NaWMn/SiO_2$ mixed oxide, that contains two elements capable of changing their oxidation state. This catalyst was first reported in the publications of the Lanzhou Institute of Chemical Physics (China) [4, 5]. Despite a significant number of published studies, the structure of active sites, as well as the role of each element in this catalytic system, are still under discussion [6]. Nevertheless, there is no doubt that further improvement of the efficiency of the system under consideration requires the development of reasonable notions about the mechanism of its catalytic action.

Earlier, we demonstrated that the kinetics of the OCM product (ethane and ethylene) formation over $NaWMn/SiO_2$ catalyst, can be described in the framework of Mars–Van Krevelen redox scheme [7], which assumes a cycling reduction and re-oxidation of the catalyst active sites. It was also revealed that this catalyst contains two forms of reactive lattice oxygen [8]. The "strongly-bonded" oxygen can be reversibly removed by the reduction the catalyst with methane and hydrogen at temperatures above 600°C, while the "weakly-bonded" oxygen releases in the TPD mode at temperatures above 650°C.

The desorption of oxygen from the $NaWMn/SiO_2$ oxide at temperature programmed heating was also described in [9–12]. Moreover, the presence of the weakly-bonded oxygen in this mixed oxide has been confirmed by the results obtained in [13], where the catalyst reduction was observed in vacuum at 800°C

during the TAP (Temporary Analysis of Products) experiments.

It was demonstrated [8] that the lifetime of the weakly-bonded oxygen at typical OCM temperatures exceeds by far the characteristic time of its reaction with methane, while the rate of methane oxidation by this type of oxygen is several times higher than by the strongly-bonded oxygen. Overall, the data presented in [8] indicated that the weakly-bonded form can be responsible for the catalytic activity via the redox OCM mechanism.

The comparison of the amounts of two forms of active lattice oxygen in a fully oxidized catalyst and the amounts of manganese and tungsten indicates that the removal of the strongly-bonded oxygen can be associated with the reduction of W^{6+} ions. However, it seems important to better understand what cations are associated with oxygen, involved in the catalytic process. One of the ways to find out is to measure the values of the binding energies of two different oxygen species. The thermochemical data can also be useful for the development and analysis of the OCM kinetic model, particularly for the evaluation of kinetic parameters of elementary reactions between various gas species involved in the OCM and the active sites of the catalyst [14–16].

The aim of this work is to determine the thermochemical characteristics of both forms of oxygen in the oxide lattice. Taking in account the significant differences between the binding energies of oxygen with W and Mn ions, as well as the strong dependence of energetic characteristics of oxygen on their degree of oxidation, the obtained results can shed light on the cationic environment of reactive oxygen species that could be associated with the active sites, participating in the catalytic process.

EXPERIMENTAL

Catalyst Preparation

The mixed $NaWMn/SiO_2$ oxide was obtained using an incipient wetness impregnation. The content of metals was (in wt %): 0.8 Na, 3.2 W, 2.0 Mn. The silica gel (Aldrich Davisil grade 646) was impregnated with the appropriate amount of sodium tungstate water solution and dried at 120°C for 3 h. After cooling to room temperature, the sample was impregnated with manganese nitrate solution, then dried at 120°C for 3 h, calcined at 600°C for 2 h and at 900°C for 6 h. Using X-ray powder diffraction (XRD) analysis, α-cristobalite was found to be the main phase; Na_2WO_4 and Mn_2O_3 phases were also detected. According to a low-temperature nitrogen adsorption measurement, the specific surface area of the sample is 4.1 m^2/g.

Samples containing the individual components of the mixed oxide (Na, W, Mn) and their double combinations (Na–W, Na–Mn, W–Mn) supported on silica were also prepared via incipient wetness impregnation. The precursors for Na, W, and Mn were sodium carbonate, ammonium tungstate, and manganese nitrate, respectively. As before, the catalysts were obtained by the silica impregnation with water solution of the corresponding salts, followed by drying at 120°C for 3 h, calcination at 600°C for 2 h and at 900°C for 6 h.

Experimental Conditions

Oxygen desorption in a flow of an inert gas at different temperatures. About 0.05 g of the sample was placed into a flow-type reactor. As a pretreatment procedure, the sample was exposed in oxygen flow at 700°C for 30 min, then cooled to 400°C, and finally purged with a flow of helium at the same temperature for another 30 min. After this procedure, the sample was heated (15 K/min ramping rate) to the required temperature (800, 850, or 900°C) in a flow of helium and kept for 20 min; the oxygen released from the catalyst was captured in a "5A" molecular sieve trap cooled to the liquid nitrogen temperature. After the experiment was complete, the chilled trap was heated to room temperature and the amount of oxygen evolving from the zeolite was measured using gas chromatography (GC) (Chromos GH-100).

Temperature programmed reduction (TPR). A 0.05 g sample of the catalyst was pretreated by heating to 500°C in a flow of O_2, keeping for 30 min, and cooling to room temperature. The O_2 flow was maintained throughout the experiment, and switched to the flow of argon at room temperature. The sample was then reduced in a flow of 10 vol % H_2 in argon, with the temperature raised to 900° at a rate of 10 K/min.

Differential scanning calorimetry (DSC) combined with reoxidation. The reoxidation experiments were performed in a flow quartz cell placed into the thermostatic block of the differential scanning calorimeter (Setaram Sensys DSC TG) with a heat flux sensor of the Calvet type. The reoxidation of the samples after oxygen desorption in helium flow was performed at 500–575°C, and of the samples reduced in the TPR mode at 625°C.

Sequential pulses of the oxidizing mixture (0.5 vol % O_2 in helium) were supplied onto the sample in a permanent pure helium flow. The amount of consumed oxygen was determined by the on-line GC analysis. The volumes of dosing loops (0.85 and 3.4 mL) used in the reoxidation experiments was considerably larger than the sample volume (about 0.1 mL) loaded into the quartz cell. At a 20 mL/min carrier gas flow rate, the estimated contact times of the oxidizing gas mixture with the sample for the above two loop volumes were ~2.5 and 10.2 s, respectively. Taking into account the DSC-111 calorimeter time constant $\tau \approx 25$ s, the interval between the pulses of the oxidizing mixture was set at 6 min to provide sufficient time ($\Delta t > 10\ \tau$) for the signal from the calorimetric

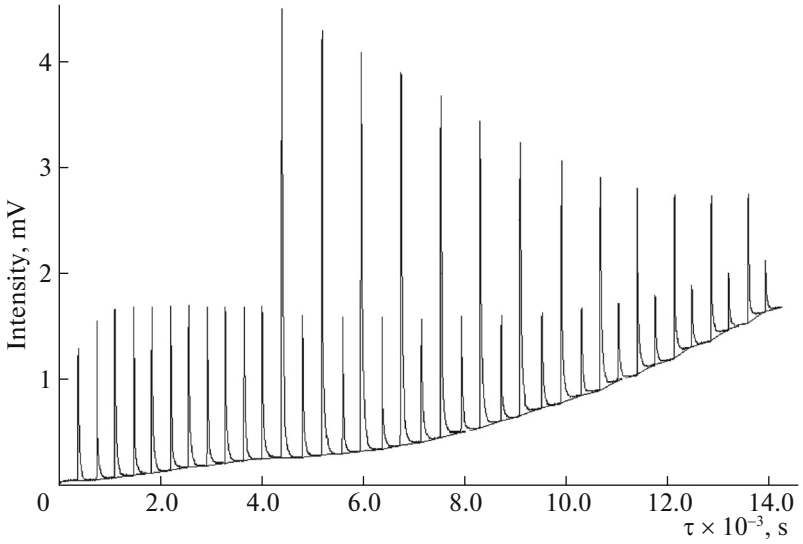

Fig. 1. Calorimetric profile for the pulse reoxidation of the NaWMn/SiO_2 sample following TPR (heating in hydrogen to 850°C).

detector to return to the horizontal base line before the next pulse supply.

The calorimeter signal base line reconstruction. Let us define the baseline of the calorimeter sensor as an idealized time-dependent signal obtained if a sample undergoes the same transformations that occur during the actual process, but in the absence of any thermal effects (heat release or consumption). In other words, the chemical composition of the sample and its physical (including thermal) properties vary, but these changes occur with zero heat effect. In the ideal case (i.e., if the sensor has no heat inertia), the shift in the calorimetric profile in respect to the zero line, which corresponds to a time-constant sensor signal, is proportional to the progress of the process leading to a change in the thermophysical properties of the sample, primarily its heat capacity:

$$\Delta U(t) \approx a\Delta C_{sam}, \quad (1)$$

where $\Delta U(t)$ is the deviation of the baseline from the zero line at time t, ΔC_{sam} is the change in the sample thermal capacity, and a is the proportionality factor.

When processing the calorimetric data obtained in this work, we encountered difficulty in calculating the heat effects due to a noticeable shifting of the baseline that occurred during the pulse oxidation of the reduced samples (Fig. 1). The shifting of the baseline results in significant errors at calculation of the heat effects, therefore, the additional analysis is required. Three algorithms for restoring the baseline are described below.

Algorithm 1. In this algorithm, the baseline is defined as a straight line that connects the last datum point on the horizontal part of the calorimetric curve, before the heat surge, and the point (real or expected) at which the curve reaches the next horizontal part. This approach does not have any theoretical basis, but the obtained value of the thermal effect can be considered as its upper estimate, since the other algorithms for the baseline reconstruction give lower areas under the calorimetric curve, as it is shown in Fig. 2.

Algorithm 2. If we assume that a pulse of molecular oxygen passes through a sample within a time considerably shorter than τ and the changes in the thermophysical properties of the sample occur on the same time scale, the baseline can be drawn as a horizontal straight line which the calorimetric signal approaches following an exponential decay. Obviously, this assumption is not quite correct even for small pulses of ~2.5 s. However, this algorithm gives us a lower estimate of the magnitude of the thermal effect.

Algorithm 3. Accounting that the measuring system responds equally fast to the changes in sample thermal capacity and to the heat release or uptake, the baseline can be reconstructed by assuming that $\Delta U(t)$ is proportional to the current area $S(t)$ under the calorimetric curve:

$$\Delta U(t)/\Delta U(t)_{max} = S(t)/S_\infty, \quad (2)$$

where $\Delta U(t)_{max}$ is the maximum shift in the baseline position at the end of the heat process and S_∞ is the total area under the calorimetric curve.

Obviously, to use Eq. (2) we must know both $S(t)$ and S_∞, but these values require a defined baseline. This contradiction can be overcome by adopting the following iterative procedure. We start, e.g., with algorithm *2* to find the first approximation to the baseline, while $S(t)$ and S_∞ determined from this baseline can be used for the next step, and so on. Using algorithm *3*, we find that the procedure converges rapidly: the difference between successive S_∞ is below 0.1% after 2–3 iterations. The obtained values lie between those

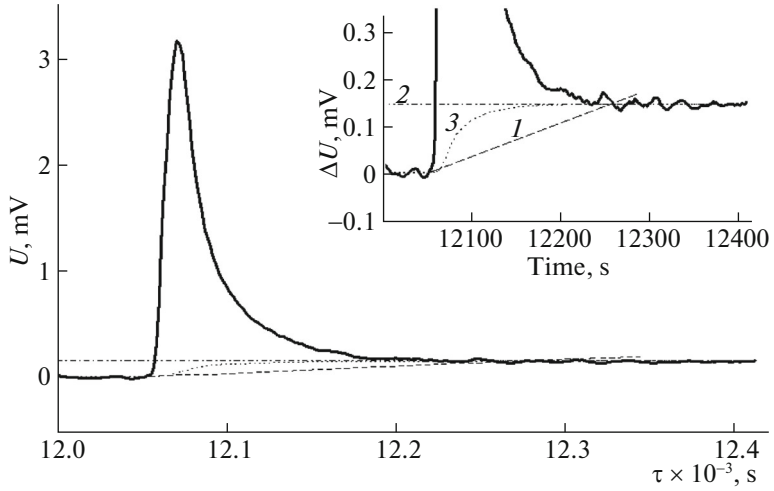

Fig. 2. Deviation of the calorimetric curve (solid line) from the zero line for the 32nd reoxidation pulse; the $NaWMn/SiO_2$ sample was preliminarily reduced by heating in hydrogen to 850°C (TPR). The insert shows the initial part of the profile in greater detail; baselines (dashed lines) (*1*), (*2*), and (*3*) were reconstructed using algorithms 1, 2, and 3, respectively (see text).

found by algorithms *1* and *2*, and seem to be a better approximation of the actual heat effects.

With the upper and lower estimates of the heat effects obtained using algorithms *1* and *2*, respectively, we were able to estimate the systematic error of the measurements associated with the uncertainty in the baseline position. In the region where the maximum shift in the baseline was observed (pulses 32–35, Fig. 1), the heat effects calculated using algorithms *1* and *3* differed by 5–6%, while for algorithms *2* and *3* the difference was 25–30%. The data presented below were obtained using algorithm *3*.

RESULTS AND DISCUSSION

Oxygen Desorption in a Flow of an Inert Gas

In the above-cited work [8], the experiments on oxygen desorption from the $NaWMn/SiO_2$ system were limited to a temperature of 800°C. The results of the present work revealed a remarkable increase in the volume of released oxygen when the temperature was raised from 800 to 850°C, however no oxygen release was observed when the temperature was further raised to 900°C.

The reoxidation experiments for the $NaWMn/SiO_2$ sample from which the weakly-bonded oxygen was preliminarily removed demonstrated that the sample consumed 28% of oxygen from the first pulse, with an associated heat effect of 188 kJ/mol. The amount of consumed oxygen dropped with each following pulse. As it can be seen from the data in Fig. 3, the heat effect remained nearly unchanged during the first seven pulses and decreased slightly thereafter. This can be attributed either to processes occurring at energetically different lattice centers or to changes in the lattice energy as reoxidation proceeded.

As it was mentioned above, the amount of oxygen that can be removed by desorption depends on the final heating temperature. The heat effect of oxygen consumption in the first pulse was found to be independent of the desorption temperature. This observation suggests that in the temperature range of 800–900°C, which corresponds to the optimum performance of the $NaWMn/SiO_2$ catalytic system, the lattice oxygen desorbs from the centers having identical cationic environments.

By varying the reoxidation temperature, we found that the amount of oxygen consumed in the first pulse increased with the temperature (Table 1), which indicates the activated nature of the process. At the same time, the heat effect per 1 mol of consumed oxygen was independent of the reoxidation temperature. The

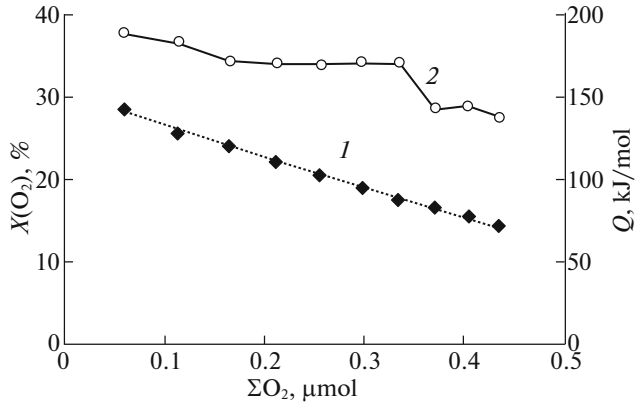

Fig. 3. Reoxidation of the $NaWMn/SiO_2$ sample following the desorption at 850°C: (*1*) oxygen conversion in a single oxygen pulse $X(O_2)$ and (*2*) associated heat effect Q of reoxidation (per pulse) vs. the integrated amount of oxygen consumed by the sample.

Table 1. The effect of the final temperature of the thermal treatment in inert gas on the amounts of released oxygen

T, °C	n_{O2}, μmol/g
800	34.5
850	56.3
900	56.4

Table 2. Effect of the temperature of reoxidation on the amount of oxygen consumed during the first pulse (A_{O_2}), and the associated heat effect of reoxidation (Q)

T, °C	A_{O_2}, %	Q, kJ/mol O_2
500	21	178
525	28	188
550	40	186
575	49	183

Table 3. Calculated heat effects per 1 mol of consumed oxygen, of the formation of different manganese and tungsten oxides

Entry no.	Reaction	Valency change	Q, kJ/mol O_2
1	$W + O_2 \rightarrow WO_2$	$W^0 \rightarrow W^{4+}$	588
2	$2WO_2 + O_2 \rightarrow 2WO_3$	$W^{4+} \rightarrow W^{6+}$	506
3	$6MnO + O_2 \rightarrow 2Mn_3O_4$	$Mn^{2+} \rightarrow Mn^{3+}$	465
4	$4MnO + O_2 \rightarrow 2Mn_2O_3$	$Mn^{2+} \rightarrow Mn^{3+}$	375
5	$4Mn_3O_4 + O_2 \rightarrow 6Mn_2O_3$	$Mn^{2+} \rightarrow Mn^{3+}$	196
6	$2Mn_2O_3 + O_2 \rightarrow 4MnO_2$	$Mn^{3+} \rightarrow Mn^{4+}$	171

activation energy E_a can be estimated from the data shown in Table 2. The data in Fig. 3 demonstrate that oxygen conversion drops linearly with the amount of oxygen consumed by the mixed oxide, indicating that the order of the reaction with respect to the concentration of reduced centers is close to 1. Assuming also the first order with respect to gaseous O_2 and using the data from Table 2, the activation energy was estimated to be 19.2 kJ/mol, Such a low E_a along with a quite high temperature required for this process are indicative of a complicated mechanism of the process. Reoxidation is likely to follow a stage that proceeds only at rather high temperatures.

Thus, based on the experimental data, we estimated the heat effect of reoxidation due to the formation of the weakly-bonded form of lattice oxygen in the mixed oxide system $NaWMn/SiO_2$. It has averaged 185 kJ/mol O_2. Using this value, the binding energy $E_{(Me-O)}$ of the lattice oxygen can be estimated. Let us assume that the heat effect does not include the energy of lattice reconstruction; i.e., that oxygen turnover does not modify the phase composition of the oxide and involve only the formation and refill of oxygen vacancies:

$$MeO_X \rightarrow MeO_{X-1}[\,] + 1/2O_2, \qquad \text{(I)}$$

where [ ] is an oxygen vacancy. $E_{(Me-O)}$ can then be calculated using the equation

$$E_{(Me-O)} = [Q_{reox}(1) + D(O_2)]/2, \qquad (3)$$

where $Q_{reox}(1)$ is the heat released per mole of the consumed O_2, and $D(O_2)$ is the dissociation energy of molecular oxygen.

The value of $E_{(Me-O)} = 337$ kJ/mol, was calculated using Eq. (3) for oxygen desorption at temperatures up to 900°C. Considering the pronounced differences between the energy characteristics of oxygen in manganese and tungsten oxides, the obtained value of the oxygen binding energy allowed us to make reasonable assumptions regarding the cations that changed their oxidation state during the catalyst reoxidation. Table 3 summarizes the heat effects of formation of manganese and tungsten oxides, which were calculated based on the reference data for the standard heats of formation for these oxides [17].

As it can be seen, the heat effect of oxygen binding in manganese oxides is affected not only by a change in the manganese oxidation state, but to a great extent by modifications in the oxide lattice structure that accompany this process. Despite the chemical process being nominally the same for reactions (3)–(5), i.e.,

$$2Mn^{2+} + 1/2O_2 \rightarrow 2Mn^{3+} + O^{2-},$$

there are considerable differences between the values of the reaction heat effects. These differences are attributed to variations in the structures of these oxides, meaning that the heat effect for each reaction includes an associated change in the crystal lattice energy. Since the formation of hausmannite (Mn_3O_4) from MnO and Mn_2O_3 is exothermic, we would expect that it has a higher lattice energy than oxides, in which manganese formally has a single degree of oxidation: (2+) in MnO and (3+) in Mn_2O_3. Therefore, reaction (3), in which-a stable structure of hausmannite forms, exhibits a higher heat effect than reaction (5), in which hausmannite transforms to Mn_2O_3.

If the reoxidation of $NaWMn/SiO_2$ was isomorphic, i.e., with no modifications in the crystal lattice around the sites with Mn cations that change their oxidation state, the heat effect due to the oxidation of Mn^{2+} to Mn^{3+} would have had a value between the heats of reactions (3) and (5), i.e., above 196 kJ/mol O_2. The experimentally determined heat effect of the refill of weakly-bonded oxygen in $NaWMn/SiO_2$ (around 185 kJ/mol) in this case most likely corresponds to the oxidation of Mn^{3+} to Mn^{4+}. But if the structure of the mixed oxide changes within a single cycle of oxygen release and uptake, the value obtained for the heat of reoxidation requires a more complex

interpretation. Indeed, in this case a more complicated that reaction (I) process must proceed, namely

$$(MeO_X)_I \rightarrow (MeO_{X-1})_{II} + 1/2O_2. \quad (II)$$

The associated heat effect (per 1 mol of molecular oxygen) can be calculated using the following equation

$$Q_{reox}(2) = -2\Delta H(2) = -2[\Delta H_f(MeO_{X-1}) - \Delta H_f(MeO_X)], \quad (4)$$

where ΔH_f is the enthalpy of formation of the oxides, which differ in their stoichiometric composition and crystal phase structures. It should be mentioned that the values given in Table 3 were calculated using Eq. (4). By comparing Eqs. (3) and (4), we can see that Q_{reox}(I) and Q_{reox}(II) have different energy-related parameters and thus can yield different results.

This means that the heat effects calculated using the reference values for enthalpies of formation of individual oxides generally cannot be used to estimate the binding energy of lattice oxygen which participates in heterogeneous catalytic reactions proceeding via redox mechanism. Depending on the relative stability of the forming crystal lattice compared to the initial one, the value calculated using Eq. (3) can be either upper or lower estimate of the oxygen binding energy, which can affect the activation parameters of different stages in the Mars–Van Krevelen mechanism.

The obtained value of the oxygen binding energy, ~185 kJ/mol, is close to the heats of reactions (5) and (6) (Table 2), which correspond to the oxidation processes $Mn^{2+} \rightarrow Mn^{3+}$ and $Mn^{3+} \rightarrow Mn^{4+}$, respectively. The minimum temperature for oxygen desorption was 575°C, which is close to the temperature of MnO_2 decomposition (550°C) [17], indicating that the measured heat effect of reoxidation could be attributed to $Mn^{3+} \rightarrow Mn^{4+}$ oxidation process. However, the available literature data [6, 11, 18] and our data in [8] demonstrate the presence of the Mn_2O_3 phase in oxidized $NaWMn/SiO_2$ sample, suggesting that the measured heat effect is more likely associated with the process $Mn^{2+} \rightarrow Mn^{3+}$.

Temperature Programmed Reduction (TPR)

The TPR curve characterizing the reduction of the $NaWMn/SiO_2$ sample has two peaks due to hydrogen consumption (Fig. 4). The first one, in the temperature range of 500–700°C, corresponds to consumption of 97 μmol/g of hydrogen. For the second one, covering the temperatures from 700 to 850°C, the consumption of H_2 was 443 μmol/g. In the case of the sample preliminary heated in a flow of argon to 850°C, the first peak (at lower temperatures) wasn't detected during subsequent reduction. This allows us to conclude that the reduction at 500–700°C leads to the removal of a weakly-bonded form of oxygen, which, as was shown above, can also be removed upon desorption in helium. The obtained experimental results on the TPR of $NaWMn/SiO_2$ are in good agreement with [12, 18–20], which also reported two temperature ranges close to those observed in this study. Therein it is believed that the first and the second peaks on the TPR profiles were most probably due to the reduction of manganese and tungsten cations, respectively. If we assume that all the manganese in the sample was oxidized to the (3+) state at the pretreatment stage (exposure to oxygen at 500°C), the amount of hydrogen consumed during the reduction at the temperature range of the first TPR peak corresponds to the reduction of Mn^{3+} to Mn^{2+}.

Since the first TPR peak was attributed to the same $Mn^{3+} \rightarrow Mn^{2+}$ process, which was supposed to occur during the oxygen desorption experiment, with some uncertainty, the unambiguous assignment of the second reduction peak could hardly be made, based solely on data on the amount of hydrogen consumed. Processes associated with the second peak could be the reduction of manganese and tungsten, $Mn^{3+} \rightarrow Mn^{2+}$ and $W^{6+} \rightarrow W^{4+}$, or the reduction of tungsten alone, $W^{6+} \rightarrow W^{5+}$ and to some extent $W^{4+} \rightarrow W(0)$.

The TPR of the $NaMn/SiO_2$ sample consisted of two stages as well. The TPR profile (Fig. 4) has two hydrogen consumption peaks: one at 400–550°C and the other at 600–800°C; the amount of consumed hydrogen was 60 and 130 μmol/g, respectively. With sodium excluded from the oxide composition, the amount of hydrogen consumed at the 400–550°C increased notably (to 103 μmol H_2/g), and no hydrogen consumption was detected upon a further increase in temperature (Fig. 4). Therefore, we may conclude that when sodium is omitted, the temperature range of manganese reduction shifts and the total amount of consumed hydrogen is increased. It is interesting to note that the amount of hydrogen consumed by $NaMn/SiO_2$ at 600–800°C corresponds to the amount of oxygen which can be released from $NaWMn/SiO_2$ upon oxygen desorption. Meanwhile, no hydrogen consumption was observed in the same temperature range for a $NaMn/SiO_2$ sample after the pretreatment in an argon flow at temperature up to 850°C.

The TPR profile for the NaW/SiO_2 sample exhibits two hydrogen consumption peaks (Fig. 4): one at 500–600°C and the other at 600–850°C; the amounts of consumed hydrogen were 10 and 373 μmol/g, respectively. Assuming that tungsten in the sample was entirely oxidized to the (6+) state during the preliminary treatment (exposure to oxygen at 500°C), the amount of consumed hydrogen is comparable to the reduction of W^{6+} to W^{5+} and W^{4+}, and to a notable extent to W(0).

Likewise Mn-containing samples, the addition of sodium ions changed the character of the reduction of W ions. As it can be seen from the data in Fig. 4, the reduction of W/SiO_2 at 600–850°C is a complex two-

stage process, while the total amount of consumed hydrogen is increased to 410 μmol/g.

Reoxidation Following TPR

The complete consumption of oxygen was observed in the first 11 pulses upon reoxidation at 625°C of the $NaWMn/SiO_2$ sample that was treated with hydrogen in the TPR mode at 850°C; the averaged value of heat effect of oxygen uptake was 330–350 kJ/mol. During these 11 oxygen pulses, the degree of the sample oxidation reached ~17%. In order to increase the rate of oxidation, the system was equipped with an additional valve with a loop of increased size (4 times greater than the first one). The pulses from the larger and smaller loops were delivered to the sample alternatingly. The heat effect of oxygen uptake remained at approximately the same level for the reoxidation of the sample in the range of 17 to 55%; as the reoxidation progressed, it slightly decreased to about 300 kJ/mol for the sample oxidized by 85%. It is interesting to note that the amount of oxygen consumed from larger pulses was always lower than that from smaller pulses for the same values for specific heat of oxygen consumption in both cases. This observation can be explained by assuming that a limited number of sites of primary chemisorption are available on the oxide surface, and the time required to vacate them through, e.g., for the redistribution of the consumed oxygen atoms to other surface (or subsurface) sites, is longer than the time of passage of a single oxygen pulse. However, the interval between two consecutive pulses could be sufficient for such redistribution, and thus the number of centers for the primary capture of oxygen increases again before the next pulse is supplied.

As we noted above, a complex profile of the base line was observed upon reoxidation of the pre-reduced sample in the pulse mode (Fig. 1). Although the interval between two consecutive pulses was sufficiently long to allow the calorimetric profile to decay to a constant value, the latter changed with each consecutive pulse. This behavior definitely shows that the sample changed its thermal capacity upon reoxidation—likely as a consequence of some changes in its phase composition, which is not surprising for an oxide system subjected to deep reduction. It is also noteworthy that larger shifts in the base line position were observed at a later stage of reoxidation, rather than at the beginning of the process, when the consumption of oxygen was most intense.

Lowering the temperature of reduction of the $NaWMn/SiO_2$ sample to 700°C led to a notable decrease in oxygen consumption, which dropped from 42% during the first pulse to 19% during the 10th pulse. It is interesting to note that the heat effects of oxygen consumption (~190 kJ/mol), as determined from these measurements and in oxygen desoption

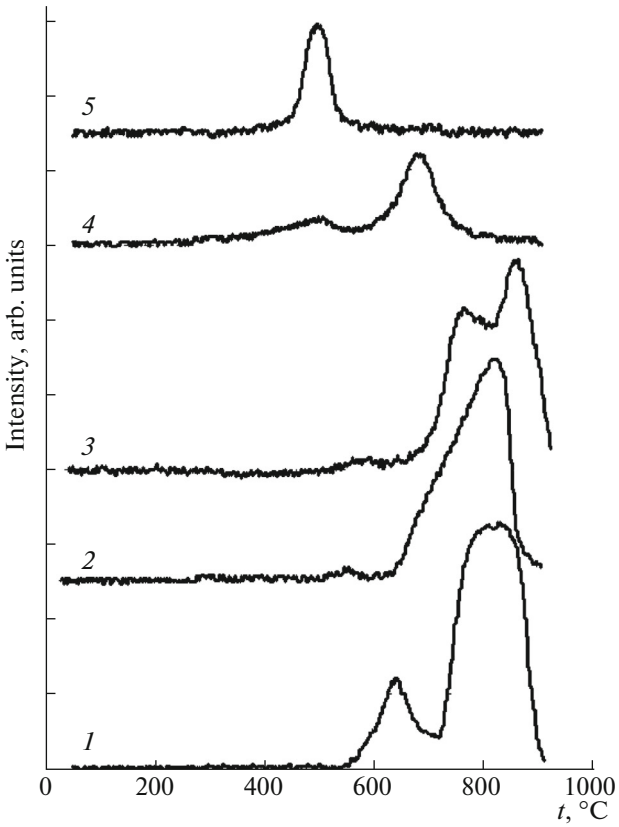

Fig. 4. TPR experiments for (*1*) $NaWMn/SiO_2$, (*2*) NaW/SiO_2, (*3*) W/SiO_2, (*4*) $NaMn/SiO_2$, and (*5*) Mn/SiO_2 samples.

experiments (see above), were the same. This observation confirms the assumption that, upon reduction at temperatures below 700°C, the catalyst released only weakly-bonded oxygen.

During reoxidation of the NaW/SiO_2 sample, the amount of oxygen consumed in each pulse dropped from 100 to 85% over the first eleven pulses, after which the degree of the sample oxidation reached ~22%. As before, the sample was reoxidized by larger and smaller pulses of molecular oxygen. The heat effect due to consumption of oxygen remained constant, around 400 kJ/mol. It decreased drastically from ~400 to ~360 kJ/mol when the degree of reoxidation reached 28%; the next notable drop in the heat effect, to ~320 kJ/mol, was observed when reoxidation of the sample progressed to 56%.

The characteristic features of the pre-reduced $NaMn/SiO_2$ sample reoxidation were similar to those noted upon reoxidation of the $NaWMn/SiO_2$ sample after oxygen desorption at 850°C (see above). The difference was observed only for the first pulse, which was characterized by a considerable consumption of O_2 (95%) and relatively high heat of consumption (272 kJ/mol). However, only 31% of the oxygen was consumed during the second pulse, and the associated

heat effect decreased to 169 kJ/mol O_2. The obtained experimental results suggest that only a small fraction of manganese ions was reduced to Mn^{2+} under these conditions (i.e., reduction in 10% H_2 at 850°C); the oxidation of these ions occurs with high heat effects in the first pulse. In the reduced sample, the manganese was mainly in the form of Mn^{3+}.

Thus, the thermochemical properties of lattice oxygen in the mixed oxide system $NaWMn/SiO_2$ were determined. The amount of weakly-bonded oxygen in the catalyst was found to be 56 μmol/g, and the experimentally measured heat effect of reoxidation was around 185 kJ/mol. Previous results demonstrated that the weakly-bonded form of oxygen has a dominate contribution to the overall rate of the OCM reaction [8]. Based on the analysis of the results obtained in this study we made an assumption regarding the possible cationic environment of the oxygen in catalytically active sites. The obtained values of binding energy suggest that the evolution of oxygen upon heating to 800–900°C could be accompanied by the reduction of manganese ions, either from (4+) to (3+) or from (3+) to (2+).

The second form of oxygen present in the oxide system under study was characterized by a higher binding energy; this oxygen can be removed from the catalyst via reduction with hydrogen (TPR) at temperatures of 700–900°C. The amount of this oxygen (443 μmol/g) and the associated heat effect of reoxidation (344–360 kJ/mol) are indicative of its binding to tungsten present in the catalyst.

A considerable shift in the position of the baseline on the calorimetric curves during reoxidation indicates a significant change in the heat capacity and some structural changes accompanying the reduction and reoxidation processes. However, it is not possible to conclude which transitions and structural changes are responsible for the removal and consumption of this form of oxygen without additional studies using structurally sensitive physical techniques. Nevertheless, it can be stated that the binding energy of this form of oxygen is so high that it can play only a minor role in the OCM reaction under steady state conditions, i.e. in the presence of O_2 in the gas phase, even in small concentrations.

ACKNOWLEDGMENTS

This work was supported by the Russian Foundation for Basic Research, project no. 16-33-50273 mol_nr, and as part of the State Assignment, project no. 0303-2016-0013, from the Boreskov Institute of Catalysis, Russian Academy of Sciences and the RF Ministry of Education and Science.

REFERENCES

1. G. E. Keller and M. M. Bhasin, J. Catal. **73**, 9 (1982).
2. O. V. Krylov and V. S. Arutyunov, *Oxidative Transformations of Methane* (Nauka, Moscow, 1998) [in Russian].
3. U. Zavyalova, M. Holena, R. Schlögl, and M. Baerns, ChemCatChem **3**, 1935 (2011).
4. X. P. Fang, S. B. Li, J. Z. Lin, and Y. L. Chu, J. Mol. Catal. (China) **6**, 255 (1992).
5. X. P. Fang, S. B. Li, J. Z. Lin, and Y. L. Chu, J. Mol. Catal. (China) **6**, 427 (1992).
6. S. Arndt, T. Otremba, U. Simon, et al., Appl. Catal. A: Gen. **425–426,** 53 (2012).
7. V. I. Lomonosov, Yu. A. Gordienko, and M. Yu. Sinev, Kinet. Catal. **54**, 451 (2013).
8. Y. Gordienko, T. Usmanov, V. Bychkov, et al., Catal. Today **278**, 127 (2016).
9. J. Wu, S. Li, J. Niu, and X. Fang, Appl. Catal. A: Gen. **124**, 9 (1995).
10. Y. Liu, R. Hou, X. Liu, et al., Stud. Surf. Sci. Catal. **119**, 307 (1998).
11. S.-B. Li, Chin. J. Chem. **19**, 16 (2001).
12. V. Fleischer, R. Steuer, S. Parishan, and R. Schomäcker, J. Catal. **341**, 91 (2016).
13. B. Beck, V. Fleischer, S. Arndt, et al., Catal. Today **228**, 212 (2014).
14. M. Yu. Sinev, Catal. Today **13**, 561 (1992).
15. M. Yu. Sinev, Catal. Today **24**, 389 (1995).
16. M. Yu. Sinev, Russ. J. Phys. Chem. B **1**, 329 (2007).
17. A. I. Efimov, L. P. Belorukova, I. V. Vasil'kova, et al., *Properties of Inorganic Substances, The Handbook* (Khimiya, Leningrad, 1983) [in Russian].
18. A. Palermo, J. P. H. Vazquez, A. F. Lee, et al., J. Catal. **177**, 259 (1998).
19. S. M. K. Shahri and S. M. Alavi, J. Nat. Gas Chem. **18**, 25 (2009).
20. Z. Jiang, H. Gong, and S. Li, Stud. Surf. Sci. Catal. **112**, 481 (1997).